In situ synchrotron XRD study of the reaction between H_2S and nanostructured pure and Cu-doped ZnO

Jonathan Skrzypski[a], Igor Bezverkhyy[a], Olga Safonova[b] and Jean-Pierre Bellat[a]

[a]*Laboratoire Interdisciplinaire Carnot de Bourgogne, UMR5209 CNRS – Université de Bourgogne, 9 av. A. Savary, BP47870, 21078 Dijon Cedex, France*

[b]*Swiss-Norwegian Beamline, ESRF, BP 220, 6 Rue Jules Horowitz, 38043 Grenoble Cedex, France*

Introduction

ZnO is extensively employed in the chemical industry for removing H_2S from gases used as raw materials in such important processes as methane steam reforming, ammonia and methanol synthesis [1]. Currently used absorbents are operational at 350-400°C and allow to remove H_2S down to several ppm level. Some emerging technologies like Fischer-Tropsch synthesis or low-temperature fuel cells (PEMFC) impose more stringent requirements on the purity of the gases (< 0.1 ppm S). This fact and necessity to use low temperatures for H_2S elimination (150-250°C), at which classic ZnO-based sorbents are not efficient, directed the research activity towards utilization of nanostructured ZnO promoted with various transition metals [2-11]. These materials, especially Cu-containing ones, were shown to possess better performance in H_2S absorption, but the mechanism underpinning the increase of the reactivity has not yet been elucidated. A better understanding of this mechanism will obviously be helpful in developing novel sorbents for H_2S removal. In our study we tried to fill this gap using *in situ* synchrotron XRD to follow ZnO → ZnS transformation both for pure zinc oxide and for Cu-containing sorbents.

Experimental

Cu-doped ZnO sorbents were synthesized by coprecipitation of $Zn(NO_3)_2 \cdot 6H_2O$ and $Cu(NO_3)_2 \cdot 2.5H_2O$ (reactive grade, Aldrich) by sodium carbonate. Coprecipitation was done at room temperature by a dropwise addition of 0.2 M solution containing Cu and Zn nitrates to a stoichiometric amount of 0.5 M solution of Na_2CO_3 under vigorous stirring. Obtained suspension was stirred for 4h, and then the precipitate was filtered, thoroughly washed with water and dried in oven overnight at 100°C. Thus obtained solid (without any grinding) was annealed in air flow at 400°C for 4 h (heating rate - 2°C/min). After calcination the solids were ground and sieved to obtain the fraction of 90-125 μm, which was used in all experiments. The pure ZnO sample was prepared in the same way without adding dopant. Composition and textural properties of the samples used in the study are summarized in Table 1.

Table 1

Sample	Molar ratio Cu/Zn	S_{BET}, m^2/g	D(ZnO), nm
ZnO		29	25.2
Cu3-ZnO	0.030	44	14.5
Cu6-ZnO	0.064	45	14.0

It should be noted that measured specific surface areas are lower than those calculated from particle size derived from XRD. This effect is due to aggregation of ZnO nanoparticles: as it follows from SEM and TEM the monocrystalline grains form tight aggregates of 70-80 nm.

The experiment was done at BM01B beamline using the high-resolution powder diffractometer. All the measurements were performed at the wavelength of 0.5 Å. The sample powder (*ca.* 5 mg) was placed inside the capillary plug flow reactor (1 mm quartz capillary with 20 μm walls) and connected to the gas source and the exhaust. The experiment was done at the atmospheric pressure. Gas blower oven was used to control the sample temperature inside the capillary. All samples before reaction were heated at 350°C in the flow of N_2 for 1h. After this step the sample was brought to the chosen temperature and then the reaction mixture containing 500 ppm of H_2S in H_2/N_2 (50/50) flow

was introduced in the reactor. The acquisition time per one XRD spectrum was 12 min. The XRD patterns were treated using the *FullProf* software package [12].

Results and discussion

Sulfidation of pure ZnO

Two series of XRD patterns representing transformation of pure ZnO into ZnS are given in Fig.1. The XRD pattern of the product obtained after a complete sulfidation contains the maxima characteristic of both cubic (sphalerite) and hexagonal (wurtzite) modifications of ZnS (Fig.2). Under used conditions the thermodynamically stable modification is sphalerite, but due to the low energy of formation of stacking faults in these structures, many different polytypes with mixed stacking sequences can be formed [13]. The extreme case of this phenomenon is a random stacking of the layers which was previously observed in ZnS nanoparticles obtained in acidic solution [14]. It was shown that in such case peak (102) of wurtzite (2θ = *12.5*°) is absent and peak (103) (2θ = *16.2*°) forms a broad hump [13]. We note that the same is true for our samples (Fig.2), which means that sulfidation of ZnO results into formation of ZnS particles with a random layer stacking and not into a mixture of two phases. Therefore the pattern cannot be described as a superposition of wurtzite and sphalerite which makes the full profile Rietveld fitting inapplicable.

In order to extract the quantitative information on the particle size and phase composition of formed ZnS (sphalerite/wurtzite ratio) in pure and Cu-containing samples the following procedure was used in the study. The pattern region 2θ=8-12° was fitted with a superposition of independent peaks having a pseudo Voigt profile function. Such a procedure permits to get the desired information because this part of the pattern contains the most intense ZnO peaks ((100), (002), (101)) and those of both ZnS modifications ((100), (002), (101) peaks of wurtzite as well as (111) and (002) peaks of sphalerite). Peaks (002) of wurtzite and (111) of sphalerite are too close to be described separately that is why in the fitting procedure they were represented by one peak. The example of such fitting

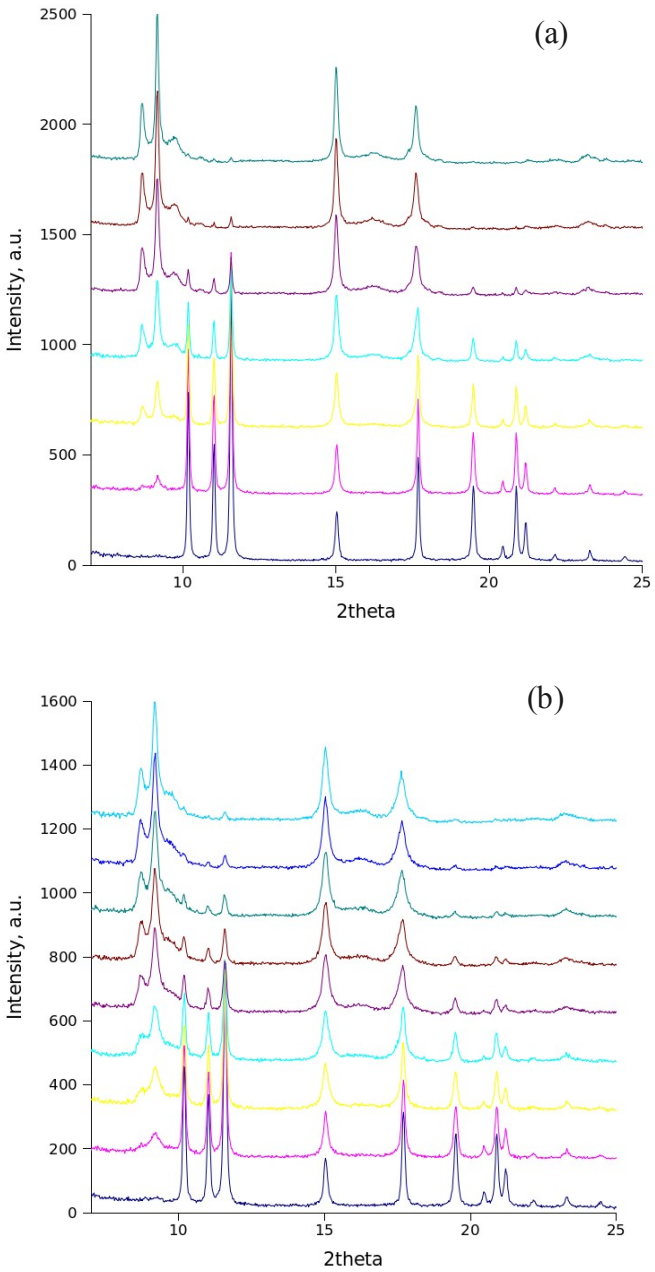

Figure 1. Series of XRD patterns recorded during sulfidation of pure ZnO at 350°C (a) and 250°C (b) (from bottom to top, time interval is 12 min for (a) and 24 min for (b)).

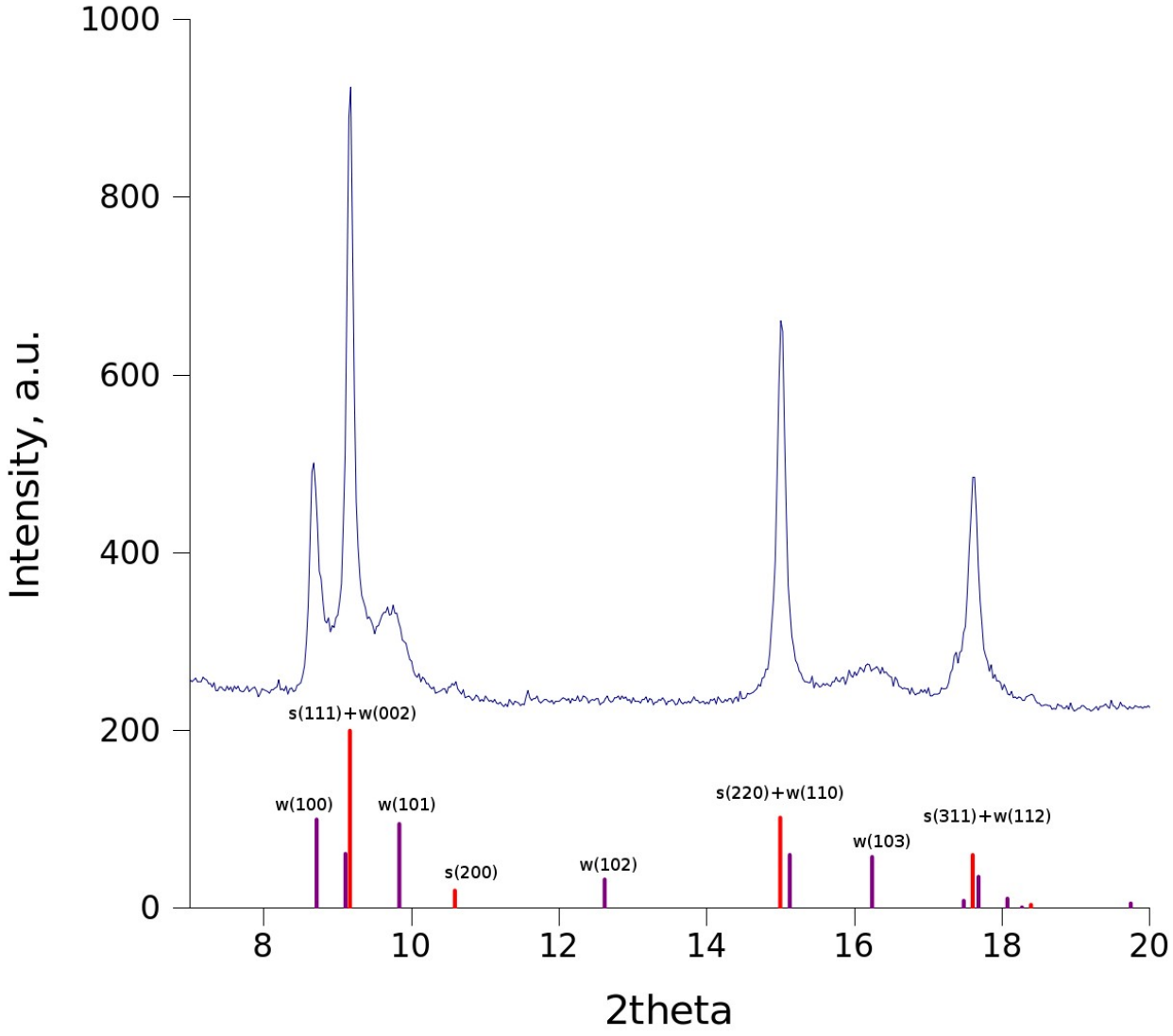

Figure 2. XRD pattern of ZnS obtained after sulfidation of ZnO at 350°C

is given in Fig.3. The integral breadths of the peaks were used to calculate the size of ZnO crystallites. The wurtzite/sphalerite ratio was calculated using the integral intensities of the peaks by means of the equation proposed in [15].

Effect of Cu on the particle size and phase composition of ZnS

The XRD patterns of Cu3-ZnO recorded during sulfidation at 250°C resemble closely those of pure ZnO (compare Fig.1 and Fig.4a). In contrast, when Cu3-ZnO sample is sulfided at 350°C and Cu6-ZnO sulfided at 250°C the XRD patterns of the formed ZnS differ significantly form those of pure ZnO (Fig.4 b,c). First, the width of the ZnS peaks strongly decreases pointing to an extensive growth of sulfide crystallites during reaction (Fig.5a). Second, we observe in these experiments a sharp drop of intensity for wurtzite (100) peak ($2\theta = 8.8°$) reflecting a decrease of the amount of wurtzite during sulfidation, so that after the complete transformation nearly pure sphalerite is formed (Fig.5b).

Both effects observed in the presence of Cu, wurtzite → sphalerite conversion and growth of sulfide crystallites, can occur only if Zn^{2+} and/or S^{2-} ions can diffuse in solid state. We conclude therefore that Cu atoms accelerate significantly the lattice diffusion in ZnS even at temperatures as low as 250°C. The origin of this unexpected phenomenon is not clear so far. Formation of sulfur anionic vacancies due to dissolution of Cu^{+1} in ZnS [16] seems not to be sufficient to explain this phenomenon, since in Cu3-ZnO these vacancies exist but at 250°C its behavior is similar to that of pure ZnO. The fact that at the same temperature the growth occurs when Cu content is higher (in Cu6-ZnO) might signify that a partial surface segregation of Cu is necessary to accelerate the transformation in ZnS particles.

Evolution of ZnO crystallite size during sulfidation

We have found that the size of ZnO crystallites during sulfidation remains constant for both pure

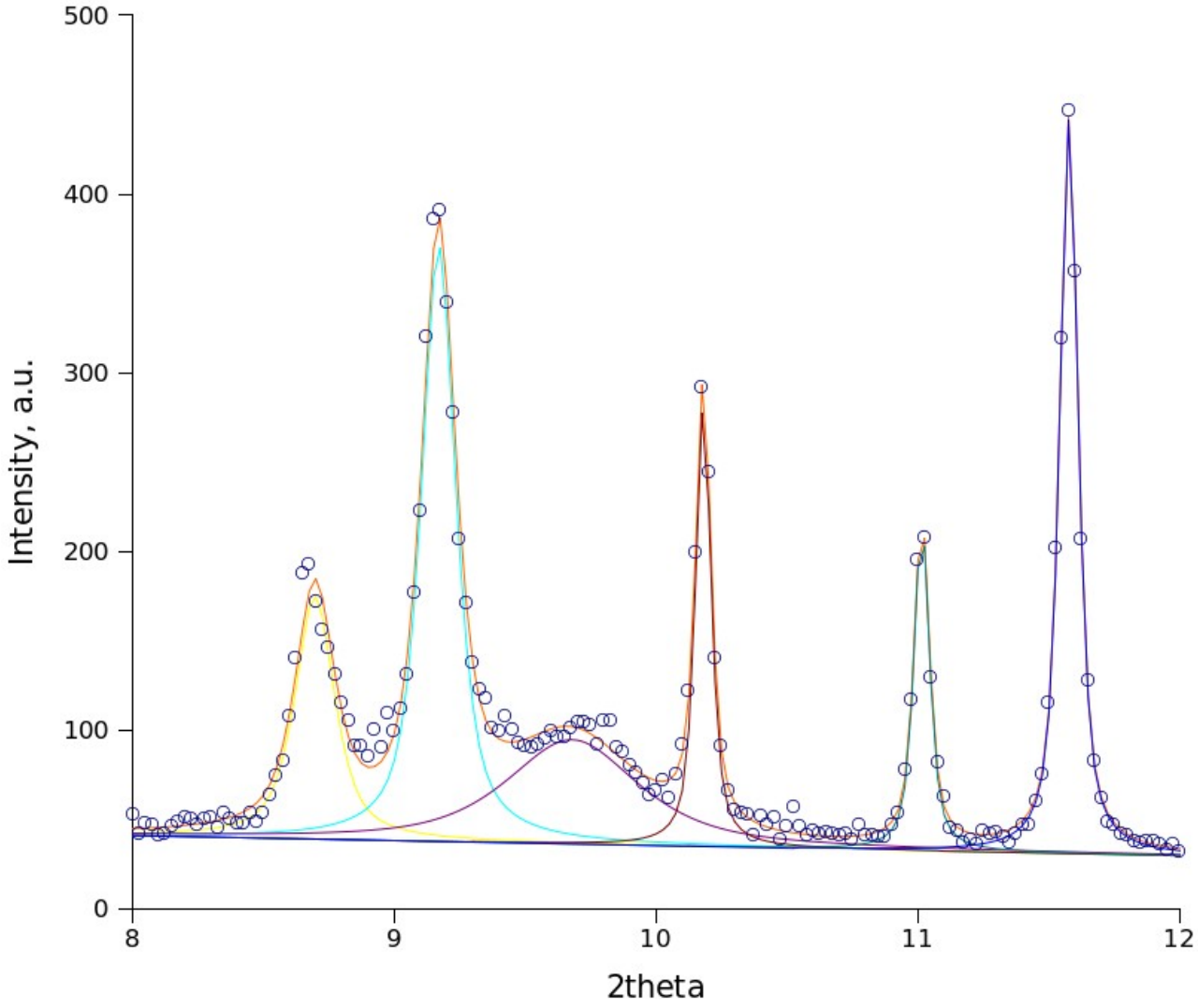

Figure 3. Description of the low angle part of XRD pattern containing both ZnO and ZnS by a superposition of single peaks.

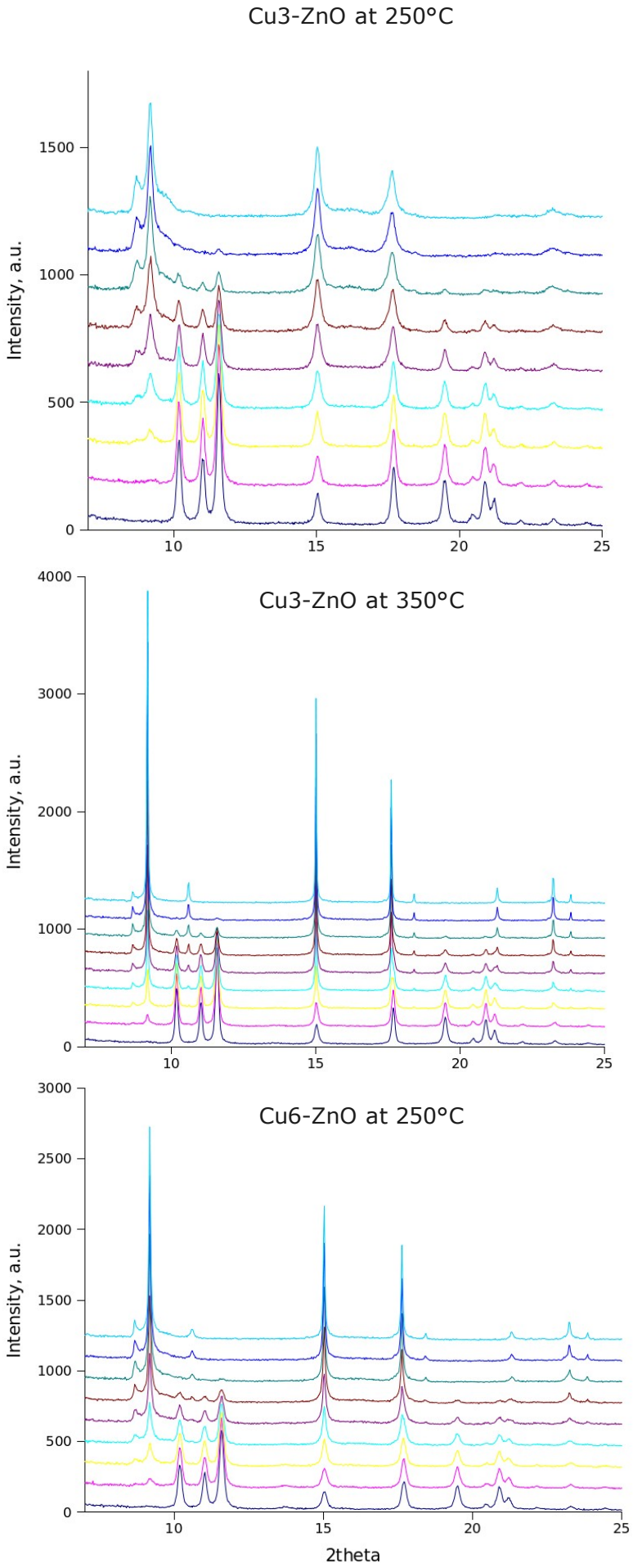

Figure 4. XRD patterns of Cu-containing ZnO samples during sulfidation (from bottom to top, time interval is 12 min).

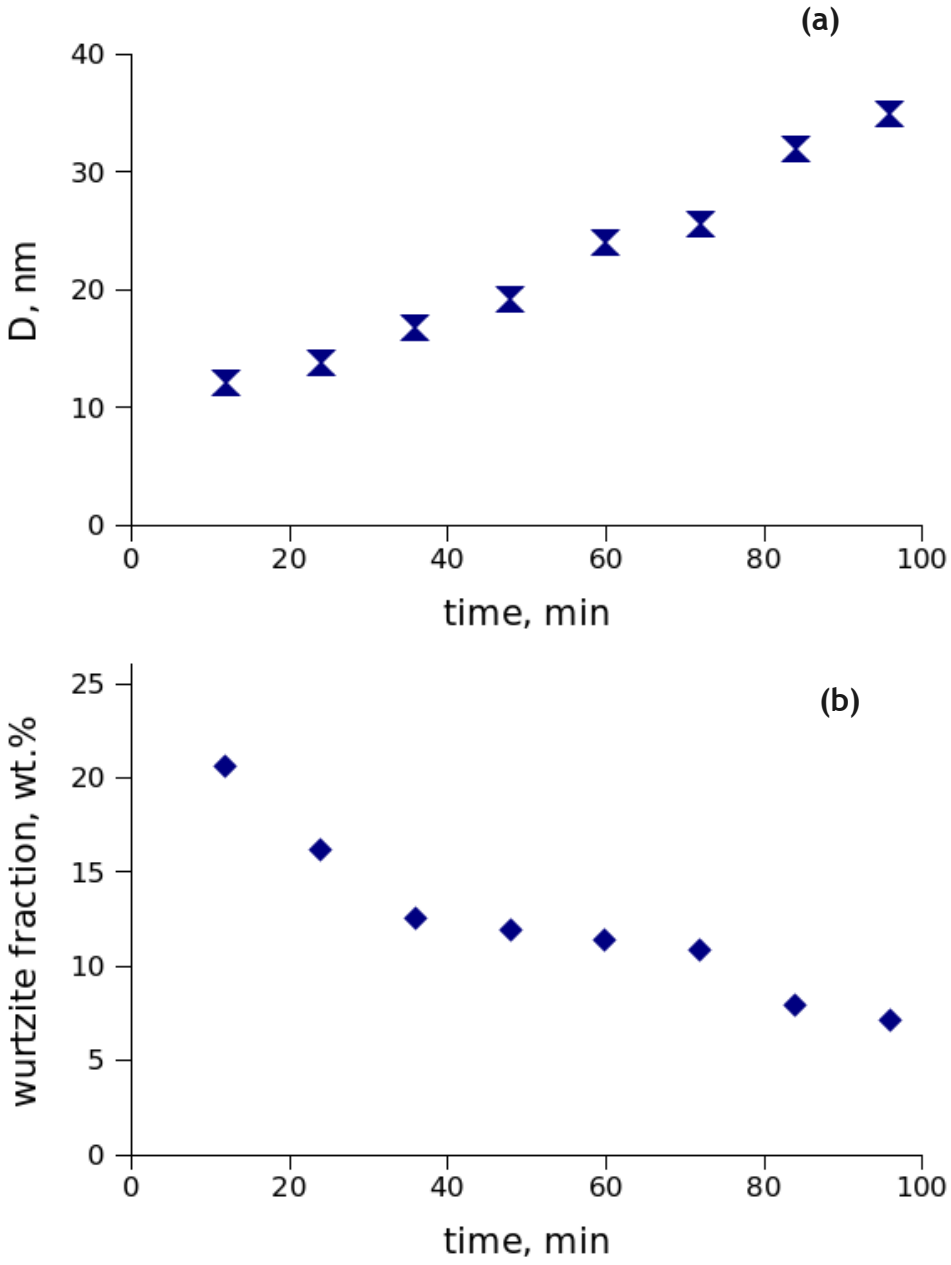

Figure 5. Evolution of sphalerite crystallite size (a) and wurtzite fraction (b) during sulfidation of Cu6-ZnO at 250°C.

and Cu-doped samples at all studied temperatures (Fig.6). This finding allowed to define the rate determining step during sulfidation of nanostructured ZnO-based sorbents. Indeed, for a gas reacting with an aggregate of crystallites two limiting cases can be distinguished [17]. In the first case, the intercrystalline diffusion of the gas (between the crystallites) is rapid while the intracrystalline diffusion (inside the crystallites) is slow and it represents therefore the rate limiting step. In this case the aggregate after partial transformation can be figured out in the following way (Fig.7) and it is obvious that the crystallite size determined from XRD in this case must decrease when reaction progresses. In the second case the crystallites in the topmost layer react rapidly (fast intracrystalline diffusion), but this transformation creates a diffusional barrier for the reacting gas and further reaction for the crystallites inside the aggregate is much slower due to insufficient gas supply. In this case it is the intercrystalline diffusion of the gas between the grains of the product which controls the overall transformation. When an aggregate is transformed according to this kinetic regime, the crystallite size of initial solid does not change during reaction (Fig.7).

The observed constancy of ZnO grain size during sulfidation points out that in our case it is the second situation which is realized. Each crystallite of ZnO can be rapidly transformed into ZnS, but the transformation of the aggregate is slow because of low diffusion rate of H_2S between the formed crystallites of ZnS and therefore insufficient gas concentration inside the aggregates. The reason of such slow diffusion of H_2S can be the plugging of the pores between the crystallites provoked by significant increase of the solid molar volume after ZnO → ZnS transformation (from 14.5 to 23.8 cm^3/mol).

Growth of ZnO crystallites in H_2 atmosphere

Taking into account the importance of ZnO based sorbents and catalysts in various domains of chemical industry, we studied also stability of ZnO nanoparticles under H_2 atmosphere. Analysis of the evolution of peak broadening in the series of XRD patterns recorded at 350°C revealed a

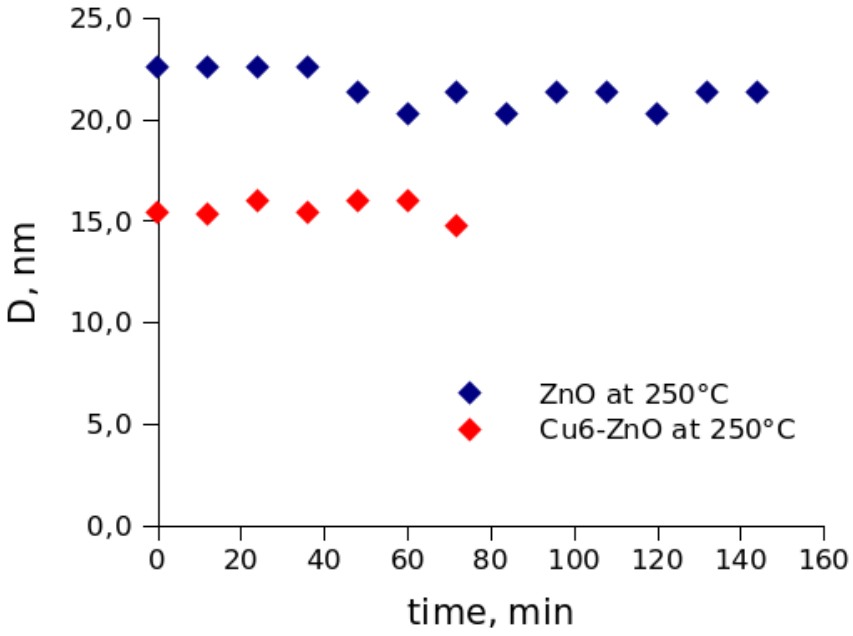

Figure 6. Evolution of ZnO crystallite size during sulfidation of pure ZnO and Cu6-ZnO.

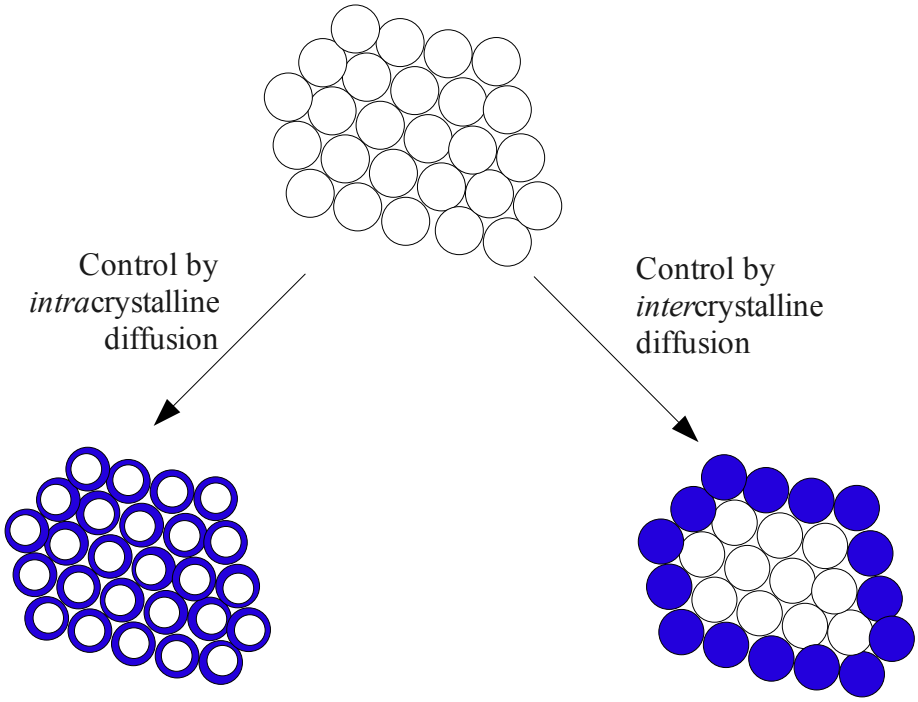

Figure 7. Two limiting kinetic regimes in the reaction between gas and an aggregate of nanoparticles (see details in the text).

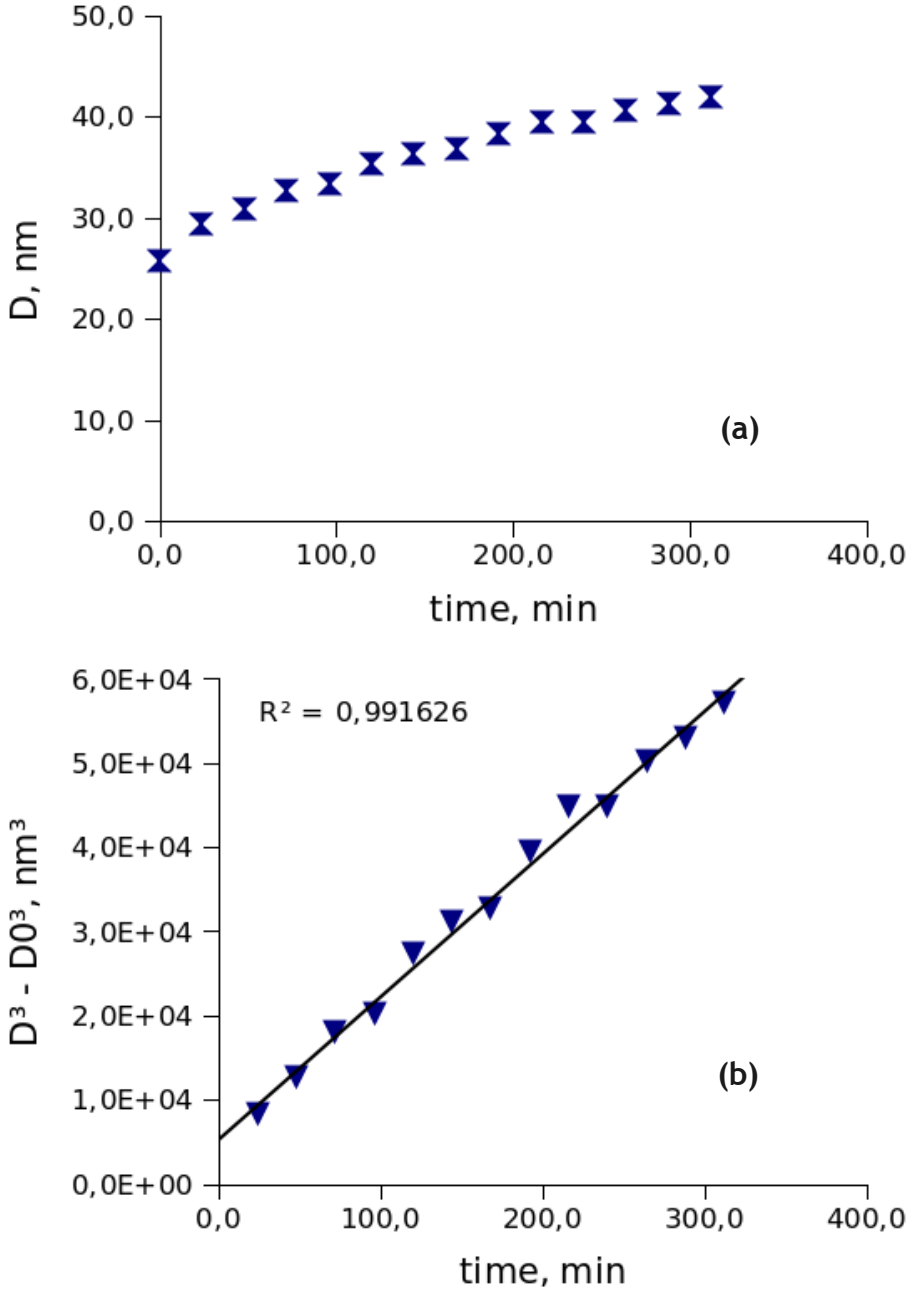

Figure 8. Evolution of crystallite size of ZnO during heating in H_2 flow at 350°C (a) and variation of cubic power of crystallite size (b).

significant increase of the crystallite size with time on stream (Fig.8a). Moreover, cubic power of the crystallite size increases linearly with time (Fig.8b), which is indicative of the Ostwald ripening mechanism [18]. Such crystallite growth, frequently observed in the colloidal systems, occurs by dissolution of smaller crystallites (due to their lower thermodynamic stability) and subsequent deposition of the matter on the larger crystallites. Its occurrence in H_2-ZnO gas-solid system is indicative of the formation of some volatile Zn-containing species which allow the matter transfer and crystallite growth. From the practical point of view this phenomenon is detrimental for the performance of ZnO-based sorbents and catalysts, because it decreases the accessible surface area of the material. Our results show that even at moderate temperatures growth of ZnO particles is sufficiently rapid and should therefore be taken into account when using ZnO-based materials in reducing atmosphere.

Conclusions

Application of *in situ* synchrotron XRD to study the reaction of H_2S with nanostructured pure and Cu-doped ZnO permitted to reveal the following features of the reaction mechanism:

i) in the presence of Cu lattice diffusion in ZnS is strongly accelerated as exemplified by wurtzite → sphalerite structural transition as well as a pronounced sintering of ZnS particles occurring at low temperature (250°C) in Cu-containing samples;

ii) the rate determining step of the sulfidation process both for pure and Cu-doped ZnO is the diffusion of H_2S between the crystallites of ZnS formed after sulfidation of the external layer of the aggregates of ZnO nanoparticles;

iii) under H_2 flow at 350°C the size of ZnO crystallites rapidly increases (following Ostwald ripening mechanism) which lowers significantly their reactivity towards H_2S.

References

1. Carnell, P. J. H. *Feedstock Purification*. In: Catalyst Handbook (Ed. M. Twigg) Wolfe Publishing Ltd, 1989.

2. Wang, X.; Sun, T.; Yang, J.; Zhao, L.; Jia, J. Low-temperature H_2S removal from gas streams with SBA-15 supported ZnO nanoparticles. *Chem. Eng. Journal* **2008**, *142*, 48.

3. Yang, H. Y.; Lu, Y.; Tatarchuk, B.J. Glass fiber entrapped sorbent for reformates desulfurization for logistic PEM fuel cell power system. *Journal of Power Sources* **2007**, *174*, 302.

4. Baird, T.; Denny, P. J.; Hoyle, R.; McMonagle, F.; Stirling, D.; Tweedy, J. Modified Zinc Oxide Absorbents for Low-temperature Gas Desulfurisation *J. Chem. Soc. Faraday Trans.* **1992**, *88*, 3375.

5. T. Baird, T.; Campbell, K. C.; Holliman, P. J.; Hoyle, R. W.; Huxam, M.; Stirling, D.; Williams, B. P.; Morris, M. Cobalt-zinc oxide absorbents for low temperature gas desulfurisation. *J. Mater. Chem.* **1999**, *9*, 599.

6. Davidson, J. M.; Lawrie, C. H.; Sohail, K. Kinetics of the absorption of hydrogen sulfide by high purity and doped high surface area zinc oxide. *Ind. Eng. Chem. Res.* **1995**, *34*, 2981.

7. Xue, M.; Chitrakar, R.; Sakane, K.; Ooi, K. Screening of adsorbents for removal of H_2S at room temperature. *Green Chemistry* **2003**, *5*, 529.

8. Yang, H.; Nair, S.; Tatarchuk, B. Regenerable H_2S sorbents with high capacity and wide temperature characteristics. *Prepr. Pap.-Am. Chem. Soc., Div. Petr. Chem.* **2006**, *51*, 499.

9. Kang, S. H.; Bae, J. W.; Kim, H.T.; Jun, K. W. ; Jeong, S. Y.; Chary, K. V. R.; Yoon, Y. S.; Kim, M. J. Effective Removal of Odorants in Gaseous Fuel for the Hydrogen Station Using Hydrodesulfurization and Adsorption. *Energy Fuels* **2007**, *21*, 3537.

10. Bae, J. W.; Kang, S.-H.; Murali Dhar, G.; Jun, K.-W. Effect of Al_2O_3 Content on the Adsorptive Properties of Cu/ZnO/Al_2O_3 for Removal of Odorant Sulfur Compounds. *International Journal of Hydrogen Energy* **2009**, *34*, 8733.

11. Jiang, D.; Su, L.; Ma, L.; Yao, N.; Xu, X.; Tang, H.; Li, X. Cu-Zn-Al mixed metal oxides

derived from hydrocarbonate precursors for H_2S removal at low temperature. *Appl. Surf. Sci.* **2010**, *256*, 3216.

12. Rodriguez-Carvajal, J. *Reference Guide for the Computer Program FullProf*; Laboratoire Leon Brillouin, CEA-CNRS, Saclay, France, 2001.

13. Zhang, H.; Banfield, J. F. Identification and Growth Mechanism of ZnS Nanoparticles with Mixed Cubic and Hexagonal Stacking. *J. Phys. Chem. C* **2009**, *113*, 9681.

14. Zhang, H.; Chen, B.; Gilbert, B.; Banfield, J.F. Kinetically controlled formation of a novel nanoparticulate ZnS with mixed cubic and hexagonal stacking. *J. Mater. Chem.* **2006**, *16*, 249.

15. Huang, F.; Banfield, J. F. Size-Dependent Phase Transformation Kinetics in Nanocrystalline ZnS. *J. Am. Chem. Soc.* **2005**, *127*, 4523.

16. Kröger, F. A. *The Chemistry of Imperfect Crystals;* North-Holland: Amsterdam, 1964, p. 688.

17. Szekely, J.; Evans, J. W.; Sohn, H. Y. *Gas-Solid Reactions;* Academic Press: New York, 1976.

18. Ardell, A. J.; Nicholson, R.B. *J. Phys. Chem. Solids* **1966**, *27*, 1793.